Leibniz-Institute of Freshwater Ecology and Inland Fisheries

Transformation of redox-sensitive to redox-stable iron-bound phosphorus in anoxic lake sediments under laboratory conditions

Lena Heinrich https://orcid.org/0000-0001-8168-3365, Matthias Rothe, Burga Braun https://orcid.org/0000-0003-1241-6735, Michael Hupfer https://orcid.org/0000-0002-8878-1045

DOI
https://doi.org/10.1016/j.watres.2020.116609

Original publication date
1 February 2021

Document version
Accepted version

Published in
Water Research

Citation
Heinrich L, Rothe M, Braun B, Hupfer M. Transformation of redox-sensitive to redox-stable iron-bound phosphorus in anoxic lake sediments under laboratory conditions. Water Research. 2021;189:116609.

© 2020 This manuscript version is made available under the CC BY-NC-ND 4.0 license.

*Manuscript
Click here to view linked References

Transformation of redox-sensitive to redox-stable iron-bound phosphorus in anoxic lake sediments under laboratory conditions

Lena Heinrich[a,b], Matthias Rothe[c], Burga Braun[d], Michael Hupfer[a]

[a]Department of Chemical Analytics and Biogeochemistry, Leibniz-Institute of Freshwater Ecology and Inland Fisheries (IGB), Müggelseedamm 301, 12587 Berlin, Germany

[b]Chair of Urban Water Management, Technische Universität Berlin, Gustav-Meyer-Allee 25, 13355 Berlin, Germany

[c]German Environment Agency (Umweltbundesamt), Wörlitzer Platz 1, 06844 Dessau-Roßlau, Germany

[d]Chair of Environmental Microbiology, Technische Universität Berlin, Ernst-Reuter-Platz 1, 10587 Berlin, Germany

Corresponding author

Lena Heinrich, heinrich@igb-berlin.de

Abstract

Phosphorus (P) can be retained in mineral association with ferrous iron (Fe) as vivianite, $Fe(II)_3(PO_4)_2 \cdot 8\ H_2O$, in lake sediments. The mineral is formed and remains stable under anoxic non-sulphidogenic conditions and, therefore, acts as a long-term P sink. In laboratory experiments under anoxic conditions, we investigated whether P adsorbed to amorphous Fe(III)-hydroxide functioned as a precursor phase of vivianite when added to different sediments as a treatment. The untreated sediments served as controls and were naturally Fe-rich (559 µmol/g DW) and Fe-poor (219 µmol/g DW), respectively. The solid P binding forms analysed by sequential extraction and X-ray diffraction were related to coinciding pore water analyses and the bacterial community compositions of the sediments by bacterial 16S rRNA gene amplicon sequencing. In the treatments, within a period of 40 d, 70 % of the redox-sensitive Fe(III)-P was transformed into redox-stable P, which contained vivianite. The mineral was supersaturated in the pore water, but the presence of Fe(III)-P functioning as a precursor was sufficient for measurable vivianite formation. The composition of the microbial community did not differ significantly (PERMANOVA, $p = 0.09$) between treatment and control of the naturally Fe-rich sediment. In the naturally Fe-poor sediment, the microbial community changed significantly (PERMANOVA, $p = 0.001$) in response to the addition of Fe(III)-P to the sediment. The freshly formed redox-stable P was not retransferred to a redox-sensitive compound by aeration for 24 h until 90 % O_2 saturation was reached in the sediment slurry. We conclude that 1) Fe(III)-hydroxide bound P, resulting from oxic conditions at the sediment-water interface, is immobilised during anoxic conditions and stable even after re-oxygenation; 2) the process is

feasible within the time scales of anoxic lake stratification periods; and 3) in relatively Fe-poor lakes, Fe dosing can provide excess Fe to form the precursor.

Graphical abstract

See separate file

Key words

Iron hydroxide adsorbed phosphorus, vivianite, sink-switch, re-aeration, lake management, microbial community composition

1 Introduction

In oxic compartments of iron (Fe)-rich lakes, phosphorus (P) is bound largely to ferric Fe, Fe(III), precipitates (Berner 1981; Parsons et al. 2017). The aerobically bound P eventually reaches oxygen (O_2)-depleted conditions within the sediment. Here, P bound to Fe(III)-compounds is released because of the reduction and accompanying dissolution of the Fe particles. This is a common issue for lake management measures applying Fe (Cooke et al. 1993). In contrast, under anoxic conditions, P can be retained permanently in mineral association with ferrous Fe, Fe(II), as vivianite, $Fe(II)_3(PO_4)_2 \cdot 8\ H_2O$ (Berner 1981; Rothe et al. 2016).

In analogy to lake sediments, it has been shown that P is bound as vivianite in anaerobic digesters of Fe-dosing sewage treatment plants (Frossard et al. 1997; Wilfert et al. 2018). Previously in the wastewater treatment process, P was adsorbed to Fe-(hydr)oxides in the aerated tanks. Vivianite was, therefore, interpreted as a transformation product of Fe-(hydr)oxide adsorbed P (Wilfert et al. 2016; Zhang 2012). Further, for lake, river, and inland sea sediments, reductive dissolution of Fe-(hydr)oxide with adsorbed P has been discussed as one key process governing the formation of redox-stable P minerals such as vivianite (Hearn et al. 1983; Hupfer et al. 2019; Reed et al. 2016; Rothe et al. 2016). Several researchers have suggested or reported vivianite as a product of high Fe(II) concentrations in the presence of aqueous P in sediments, in-situ, and by soil incubation (Borch and Fendorf 2007; Postma 1980; Walpersdorf et al. 2013). However, the sink-switch of $Fe(OH)_3$-adsorbed P as a direct precursor to redox-stable Fe-bound P, such as vivianite, in lake sediments has not been investigated yet under laboratory conditions. In particular, the control of the sink-switch by microorganisms and

68 supersaturated pore water, as well as the time frame of the transformation in lake sediments
69 require further research.

70 Batch experiments with pure cultures of Fe-reducing bacteria have suggested that
71 microorganisms control the formation of vivianite (Borch and Fendorf 2007; Glasauer et al.
72 2003). In particular, direct Fe-reducers, such as *Geobacter spp*. and *Dechloromonas spp*., and
73 indirect Fe-reducers have been identified during vivianite formation in sewage sludge (Wang et
74 al. 2019; Wang et al. 2018). There is a lack of knowledge on whether and how an excess of
75 redox-sensitive Fe and P alter the bacterial community composition of sediments, and whether
76 the bacterial community controls vivianite formation in lake sediments.

77 Saturation calculations by pore water composition are applied frequently to predict the
78 occurrence of vivianite but the method often fails in field studies (Rothe et al. 2014; Rothe et al.
79 2016). This failure could be ascribed probably to small-scale heterogeneity within the pore
80 water (Davison 1993; Glasauer et al. 2003; Rothe et al. 2016), kinetic hindrance, competing
81 reactions, and failure to analyse the actual reacting species (Boers and de Bles 1991; Davison
82 1993). In addition, the cited field studies did not provide ideal conditions for a comparison of
83 saturation indices with mineral presence or absence, as there was no definite relation between
84 the timing of mineral formation and pore water sampling. We investigated this matter
85 employing laboratory experiments, which allow evaluating the pore water and solids at related
86 time steps. This approach could be more appropriate interpreting the relationship between
87 pore water concentrations and mineral formation.

88 The time scale at which vivianite nodules, typically found in sediments, form was estimated
89 to be six months or shorter (Rothe et al. 2016). However, laboratory studies with sewage sludge
90 and bacteria-inoculated soil slurries, both initially rich in Fe-(hydr)oxide bound P, suggested
91 much faster formation of vivianite, i.e. measurable within a few days (Borch and Fendorf 2007;
92 Wang et al. 2019). Still, such a short formation time could not be demonstrated from natural
93 lake sediments.

94 Moreover, it is unclear whether vivianite remains stable after re-oxygenation of sediments.
95 Re-oxygenation of anoxic sediment for example occurs through intrusion of oxygen-rich surface
96 water after seasonal mixing. Nriagu (1972) found that, in a laboratory atmosphere, blue,
97 surface-oxidised vivianite was stable almost indefinitely. However, further oxidation to
98 metavivianite or to poorly crystalline mixed valence or ferric Fe phosphate phases is not
99 excluded (Nriagu 1972; Rouzies and Millet 1993). These transformation products in turn could
100 be dissolved during anoxic conditions.

101 We hypothesise that redox-sensitive $Fe(OH)_3$ adsorbed P is transformed to redox-stable
102 vivianite bound P under anoxic and non-sulphidogenic conditions in lake sediments. In
103 laboratory experiments, we investigate the time scale, pore water conditions, the possibly
104 involved bacterial communities of the process, and the stability of the transformation product in
105 the case of re-aeration. The transformation of redox-sensitive $Fe(OH)_3$ adsorbed P to redox-
106 stable Fe-bound P offers the potential of anoxic P retention as a lake management measure
107 after Fe amendments or relying on naturally high Fe loads.

2 Methods

2.1 Sampling of lake sediments for incubation

Incubation experiments were conducted with sediments from two lakes with contrasting Fe contents. The sediment of lake Müggelsee, located in Berlin (Germany), was relatively Fe-rich (Table 1). Muddy sediment from Müggelsee (N52.43389°, E13.68195°) was sampled in June 2019 at a water depth of 1.1 m. The Fe-poor sediment of Langer See (Table 1), located southeast of Berlin (N52.24333°, E13.78805°), was sampled in July 2019 at a depth of 3.4 m. A gravity corer (UWITEC) was used to collect a total of 3 L of sediment from each lake from the upper 0 - 3 cm layer. The sediments were stored at 10 °C for less than 72 h until preparation of the experiment batches.

2.2 Preparation of $Fe(OH)_3$-P

An amorphous $Fe(OH)_3$ powder, FerroSorp® Plus (HeGo Biotec), was ground with an agate mortar, and subsequently, 20 g was suspended in a solution of ultrapure water (100 mL) with $NaH_2PO_4 \cdot 2\ H_2O$ (19.5 g). The slurry was mixed for 2 d to reach adsorption equilibrium. After centrifugation, the overlying water was removed and the $Fe(OH)_3$ powder with the adsorbed P, $Fe(OH)_3$-P, was washed nine times with ultrapure water to remove dissolved P from the solution. The washing water was analysed for P each time to estimate desorption during the washing procedure and determine the final loading of the $Fe(OH)_3$ with P (80 mg P/g $Fe(OH)_3$, molar Fe/P = 3.1). After the last wash, the $Fe(OH)_3$-P solids were suspended in 250 mL of lake water from Müggelsee.

2.3 Set-up and sampling of incubation experiments

The sediments from lake Müggelsee and Langer See were homogenised respectively by stirring and then each divided into two parts. Then, 100 mL of the $Fe(OH)_3$-P slurry was added to the treatments and 100 mL of lake water (Müggelsee) was added to the controls. Subsequently, 28 microcosm batches of each were prepared by placing 25 mL of sediment in PVC tubes, with water from lake Müggelsee poured on top up to 50 mL.

All four types of sediment (Table 1) were incubated under O_2-free conditions in a nitrogen (N_2)-filled glovebox (O_2 < 10 ppm, Labstar, MBraun) at room temperature (27 ± 2 °C, N = 24 measurements per d, TG-4100, Tinytag) for 120 d. The incubation of the sediment originating from Müggelsee started on 13 June 2019 and of those from Langer See on 29 July 2019. At each time step of sampling, four random replicates of the control and treatment tubes were examined for both lakes. At first, the overlying water was removed with a syringe, after which, the pore water was extracted with Rhizon samplers (pore size: 0.12 - 0.18 µm, Rhizosphere Research Products B.V.). The remaining solids were kept in the N_2-filled glovebox for less than 24 h until the start of solid analyses.

After the anoxic period, four replicates were removed from the glovebox and oxygenated with air bubbling from the bottom of each tube and, simultaneously, orbitally shaken (75 rpm) for 24 h until 90 % O_2 saturation was reached in the suspended sediment. Sampling was carried out in similar manner to the anoxic time steps.

2.4 Solids analyses by sequential extraction and X-ray diffraction

After removal of the pore water, the remaining sediment of lake Müggelsee was compacted. Therefore, in order to homogenize the sediment, the amount of pore water removed was replaced inside the N_2-filled glovebox by the first extractant of the fractionation scheme subsequently applied. P fractions of the homogenized wet sediments of controls and treatments from both lakes were distinguished following the three first extraction steps of the scheme published by Psenner et al. (1984) and modified by Hupfer et al. (1995). The fractions were characterised and named by the extracting agents. Loosely surface adsorbed P was released by N_2 saturated 1 M ammonium chloride (A) and redox-sensitively bound P by 0.11 M bicarbonate/dithionite (BD). Both fractions were determined after digestion of total P (TP) by potassium persulphate. The fraction dissolved by 1 M sodium hydroxide (NaOH) was distinguished further, namely the directly measured soluble reactive P (SRP) indicated P bound to, e.g. Fe oxides (Psenner et al. 1984) and vivianite (Rothe et al. 2015). The non-reactive P (NRP), calculated as TP after digestion by potassium persulphate minus the SRP concentration, showed P released from organic material. At three of the seven time steps the complete fractionation scheme was analysed with P enclosed in carbonates extracted with 0.5 M HCl and, finally, residual P released by digestion of the remaining material. For calculation of the extraction yield, the total P content of the freeze-dried and ground bulk samples was determined after wet digestion with one part H_2O_2 (30 %) and one part H_2SO_4 (5 M) at 120 °C. P was measured in the solutions with the ammonium molybdate method (DIN EN ISO 6878). Additionally, Fe released by BD was determined by atomic absorption spectroscopy (AAS pinAAcle 9001, Perkin Elmer). Sediment dry weight (DW) was determined after drying at 105 °C

and organic matter content (OM) was calculated as loss on ignition at 450 °C. Sediment contents of Fe and S were determined by inductively coupled plasma optical emission spectrometry (ICP-OES, iCAP 6000series, Thermo Scientific) after wet digestion of the freeze-dried and ground sediment samples with one part HCl (37 %) and three parts HNO_3 (65 %) in a high-pressure microwave oven (µPrep-A, MLS GmbH).

Crystalline minerals in the solid samples were characterised after freeze-drying by powder X-ray diffraction (XRD) with an X`PERT Pro PANalytical with Copper-Kα-radiation equipped with a PIXcel1D detector (Malvern Panalytical). The diffractograms were measured between 10° 2θ and 80° 2θ with a step of 0.026° 2θ, and an integration time of 720 s/step. Peak identification was carried out by QUALX2.0 (Altomare et al. 2015) using the POW_COD database (Altomare et al. 2015) derived by the Open Crystallography Database COD (Grazulis et al. 2009). Vivianite quantification was carried out by Rietveld refinement of XRD measurements, with calculation of the amorphous content by the internal standard method. Dr T. Witzke (Malvern Panalytical) measured one treatment sample from Langer See with rutile as internal standard between 6° 2θ and 75° 2θ with a step of 0.02° 2θ and an integration time of 98 s/step. Dr Witzke used an AERIS (600 W) with Cobalt-radiation equipped with a PIXcel1D detector (Malvern Panalytical), and evaluation was done with Malvern HighScore Plus 4.8. One treatment sample from Müggelsee was measured by Dr J. Dietel (Landeslabor Berlin-Brandenburg) with corundum as internal standard between 2° 2θ and 85° 2θ with a step of 0.02° 2θ and an integration time of 192 s/step. A Bruker D8 Advance with Cobalt-radiation equipped with a LynxEye detector (Bruker) was used and evaluation was carried out by BGMN/Profex.

2.5 Pore water analyses

Immediately after extraction of pore water, the redox potential (SenTix ORP, pH 330, WTW), pH, and temperature (SenTix® 41, Multi 340i, WTW) in the pore water were measured inside the O_2-free glovebox.

A sample aliquot was fixed by adding 30 µl sulphuric acid (10 N) before removal from the glovebox and was used to determine the concentrations of dissolved ferrous and total Fe photometrically by the 1,10-phenanthroline method (DIN 38406-1). The SRP concentration was determined photometrically by the ammonium molybdate method (DIN EN ISO 6878). The remaining sample fixated by sulphuric acid was stored at 5 °C until analysis of total dissolved Al, B, Ca, K, Mg, Mn, Na, and Si by ICP-OES (DIN EN ISO 11885) on an ICP iCAP 6000series (Thermo Scientific).

The dissolved anion concentrations of Cl^- and SO_4^{2-} were determined by ion chromatography (Shimadzu and Metrohm) with detection via conductivity (DIN EN ISO 10304-1). The sample container was closed inside the anaerobic glovebox and stored at 5 °C until the analysis was carried out within 24 h after sampling.

2.6 Bacterial community analysis

Bacterial community analysis was carried out before and at the second sampling after O_2-free incubation (i.e. for Müggelsee at day 13 and for Langer See at day 8). At each sampling time point, sediment samples were taken in four replicates, respectively. The solid samples were freeze-dried and stored in the dark at room temperature. The total bacterial community DNA was extracted with the GeneMATRIX Soil DNA Purification Kit (Roboklon) according to the

manufacturer's instructions but with minor adaptations. The adaptations included cell disruption carried out by a FastPrep at 4 m/s for 60 s with freezing (– 80 °C for 0.5 h) and thawing (37 °C for 0.5 h) afterwards, and using FastPrep again at 4 m/s for 20 s. Bacterial 16S rRNA gene amplicon sequencing (V3-V4) was performed by omics2view consulting GbR. The sequencing was conducted on Illumina MiSeq, v2 micro, 2 x 250 bp.

2.7 Statistics and thermodynamic calculations

The statistical tests (Wilcoxon rank-sum test) were calculated by R version 3.6.1. All results are reported as the mean and standard deviation of four replicates if not stated otherwise.

The statistical and graphical evaluation of the bacterial community composition was carried out using the R package vegan (Oksanen et al. 2013) and customised R scripts with $OTU_{0.97}$ (operational taxonomic units at a similarity level of 97 %), not considering OTU with a maximum abundance < 0.1 % for alpha-diversity measures. OTUs with a maximum abundance < 0.3 % were not considered for beta diversity as they did not add information to the statistical analysis. PERMANOVA tests were computed by the ADONIS2 function with 999 permutations on Bray-Curtis dissimilarity. SIMPER analysis with 999 permutations was used to identify OTUs contributing significantly to the dissimilarity of subsets and up to a cumulative contribution of 60 %.

The thermodynamic calculations of saturation indices were conducted by PhreeqC version 3.4.0 (Parkhurst and Appelo 2013) using the PhreeqC database. The measured pore water conditions (temperature, pH, redox potential) and the determined pore water concentrations of Al, B, Ca, Cl^-, Fe^{2+}, K, Mg, Mn, Na, SRP, Si, and SO_4^{2-} were included in the calculation. The

saturation indices were corrected after Habraken et al. (2013) by the number of growth units for vivianite (Rothe et al. 2016).

3 Results

3.1 Transformation of redox-sensitive to redox-stable solid Fe-P during anoxic incubation

Comparing the P fractions of the treatment and control samples at the start of experiments demonstrated that the additional $Fe(OH)_3$-P was recovered completely in the BD-TP fraction (Figure 1). During anoxic incubation, the BD-TP fraction decreased, whereas the NaOH-SRP fraction increased in the treatment samples from both lakes (Figure 1). As the sum of the BD-TP and NaOH-SRP fractions was stable during anoxic incubation (Figure 1), BD-TP was transformed only into NaOH-SRP and not into other binding forms. The BD-TP and NaOH-SRP contents in the control groups of both lake sediments were unchanged (Figure 1).

The sink-switch was fastest at the beginning of the anoxic incubation but afterwards flattened out (Figure 1). The major transformation from BD-TP to NaOH-SRP in the treatments occurred during the first 40 d (Figure 1). Net balances of BD-TP and NaOH-SRP on the initial BD-TP (i.e. added as $Fe(OH)_3$-P) estimated the change in the relative contribution of these binding forms in the treatment samples. In the experiment with Müggelsee sediment, 69 % of the initially added BD-TP was transformed into NaOH-SRP, whereas 36 % remained in the BD-TP fraction even after 40 d of anoxic incubation. In the sediment from Langer See, 72 % was transformed into NaOH-SRP after 37 d and 33 % remained in the BD-TP fraction. Because of differing extraction yields, the P balances of the transformation of initially added BD-TP displayed a surplus of 5 % for both lakes.

253 During the anoxic incubation of the Fe-P-amended sediments, the BD-Fe content decreased
254 consistently with BD-TP (Figure 1), so that the molar BD-Fe/BD-TP ratios remained constant
255 (Table 2).

256 **3.2 Vivianite identification by XRD and quantification at selected time steps**

257 Powder XRD showed that the Fe(II)-P mineral vivianite (COD: 9012898) was detected in all
258 replicates of the treatment sediments from both lakes after the second sampling but not at the
259 first sampling after anoxic incubation (Figure 2). The three largest vivianite peaks were
260 identifiable for the treated sediments from Langer See after 8 d and from Müggelsee after 26 d.
261 The intensity of vivianite peaks increased with time (Figure 2). In addition to vivianite, all
262 incubated replicates of the treated and control sediments from both lakes contained crystalline
263 phases of SiO_2 (COD: 1011176) and $CaCO_3$ (COD: 9016706) at all investigated time steps.
264 Further, crystalline FeS_2 (COD: 1544891) was identified in all replicates of Langer See at all time
265 steps and at most time steps in some of the control and treated sediments from Müggelsee.
266 Ammonium chloride (COD: 1011129) was an artefact of the sample preparation (see chapter
267 2.4) in the sediments from Müggelsee.

268 The vivianite content in one replicate of the treated sediment from Langer See was 6.7 %
269 after 37 d of anoxic incubation. One replicate of the treated sediment from Müggelsee
270 contained 1.3 % vivianite according to XRD after 26 d of incubation. Assuming that the increase
271 in the NaOH-SRP fraction in the treated compared to the control sediments could be ascribed
272 only to vivianite formation suggested similar values, namely a vivianite content of 4.7 % and
273 1.5 % of total dry weight in the same treatment replicates, respectively.

3.3 Pore water conditions

The treated sediments from both lakes took up SRP from the pore water during the first 20 d of incubation and, subsequently, started to release SRP (Figure 3). In contrast, the control sediments from both lakes released SRP from the beginning. Overall, the SRP concentrations in the pore water of the treatments were 50 % to 70 % lower than were those in the controls.

As regards dissolved Fe^{2+}, the concentration increased at the beginning of the experiment in both treated and control sediments from Müggelsee, subsequently formed a plateau, and decreased again after 40 d (Figure 3). The Fe^{2+} concentration was higher in the controls than in the treatments during the entire anoxic incubation period. In the treated sediment from Langer See, the Fe^{2+} concentration in the pore water showed development similar to that in the Müggelsee sediment (Figure 3). The dissolved Fe^{2+} concentration in the Fe-poor control sediment of lake Langer See was low throughout the experiment.

The saturation indices of vivianite were calculated based on pH, redox potential (Eh), and the concentrations of dissolved ions in the pore water. During anoxic incubation, the pH was at slightly alkaline conditions, with higher values in the treatments (Table 3). As provoked by the experimental design, Eh was negative in all sediment types (Table 3). Vivianite was supersaturated in the incubated sediments, except the control from Langer See (Table 3).

3.4 Bacterial community analysis

The bacterial community composition was analysed in the control and the treated sediments before anoxic incubation and at one sampling during anoxic incubation (i.e. after 8 d for Langer See and 13 d for Müggelsee).

295 The bacterial richness on species level ($OTU_{0.97}$) was estimated by Chao1 (Table 4) and was
296 not significantly different between the sediments from Langer See. After 13 days of anoxic
297 incubation, the Müggelsee sediments had a significantly higher bacterial richness than before
298 the incubation. The Simpson's Diversity Index indicated that the distribution of the bacterial
299 communities was extremely diverse in all the samples on OTU level (Table 4).

300 For all the samples, the beta-diversity of the bacterial communities measured by Bray-Curtis
301 dissimilarity (Figure 4) was the highest between the two lakes (PERMANOVA: $p = 0.001$). The
302 dendrogram displayed two distinct clusters formed between Müggelsee and Langer See (Bray-
303 Curtis dissimilarity > 0.8).

304 Within the Müggelsee cluster, samples from the start of the experiment and the second
305 sampling time point each clustered together (Figure 4; PERMANOVA: $p = 0.001$). Before
306 incubation, *Actinobacteria* and uncl. Bacteria were most abundant, whereas, under anoxic
307 conditions, additional *Proteobacteria* and *Chloroflexi* were abundant. These phyla together
308 represented more than 80 % of the microbial community composition. In the sediments
309 originating from Müggelsee, after 13 d of anoxic incubation the bacterial communities in the
310 control samples could not be distinguished significantly from those of the treated sediments
311 (Figure 4: Bray-Curtis dissimilarity < 0.3, PERMANOVA: $p = 0.09$).

312 For Langer See, two subclusters constituted of samples from treated sediment (Fe-P) and
313 non-treated sediment (control) respectively (Figure 4; PERMANOVA: $p = 0.001$). In the treated
314 sediments, *Proteobacteria*, uncl. Bacteria, *Chloroflexi*, *Actinobacteria,* and *Cyanobacteria,* and in
315 the control sediments, additionally *Acidobacteria* and *Bacteriodetes* together represented more

than 80 % of the microbial community composition. The bacterial community composition of the sediments from Langer See differed, to a minor degree, over time (Figure 4: Bray-Curtis dissimilarity < 0.3, PERMANOVA Control: $p = 0.03$, PERMANOVA Fe-P: $p = 0.03$).

The OTUs that contributed significantly and up to a cumulative contribution of 60 % to the dissimilarity in time for the Müggelsee subset were identified by SIMPER analysis (Supplementary information 1). Therefore, in the Müggelsee sediment during 13 d of anoxic incubation, the quantity of *Ilumatobacter* sp. and *Gaiella* sp. decreased, whereas the quantity of *Ignavibacterium* sp., *Thiobacillus* sp., *Vicinamibacter* sp. and *Hydrogenispora* sp. increased.

SIMPER analysis showed that the control and treatment samples of Langer See (Supplementary information 2) differed in OTUs of the phyla *Acidobacteria* (*Vicinamibacter* sp.), *Bacteroidetes* (further unclassified), *Calditrichaeota* (*Calorithrix* sp.), *Chloroflexi* (*Anaerolineaceae*), *Ignavibacteriae* (*Ignavibacterium* sp.), *Verrucomicrobia* (*Terrimicrobium* sp.), and of the classes *β-Proteobacteria* (*Rhodocyclales*), *γ-Proteobacteria* (*Chromatiaceae* and *Steroidobacteraceae*) and *δ-Proteobacteria* (*Desulfatiglans* sp. and *Sythrophaceae*). All these OTUs had lower abundance in the treated sediments than in the control samples. *Actinobacteria* (*Ilumatobacter* sp., *Rubrobacteria* and unclassified class) and *Cyanobacteria* (*Cyanobium* sp., *Nostocales* and unclassified class), as well as OTUs affiliated to the classes *β-Proteobacteria* (unclassified order) and *γ-Proteobacteria* (unclassified order) were more abundant in the treated samples. *Actinobacteria*, *Chloroflexi* (*Caldilineaceae*), *Cyanobacteria* (e.g. *Cyanobium* sp.), and *Proteobacteria* (e.g. *Thiobacillus* sp.) contributed to the dissimilarity in the treated sediments from Langer See over time (Supplementary information 3).

3.5 Stability of Fe-P bound under anoxic conditions after re-aeration

The aeration of the resuspended sediments exceeding 90 % O_2 saturation resulted in changes in the NaOH-SRP fraction. These changes were in a range of the standard deviation of the extraction yield. The NaOH-SRP fraction in the treated sediment from Langer See increased by 10 % of total P and this P fraction decreased in the Müggelsee sediment by 4 % of total P (Figure 1). The mean yields and their standard deviations were (87 ± 10) % for Langer See and (98 ± 9) % for Müggelsee. Therefore, the NaOH-SRP fraction did not change further than the yield gaps of the fractionations. The BD-TP fractions of anoxic and re-aerated treatment samples did not change significantly (Figure 1, Wilcoxon rank-sum test, Müggelsee: W = 9, p = 0.9, Langer See: W = 15, p = 0.06,). The BD-Fe contents of the treatment sediments increased because of the re-aeration and accounted for higher BD-Fe/BD-TP ratios (Table 2). This effect was observed also in the natural Fe-rich control sediment from Müggelsee but not in the Fe-poor sediment from Langer See. Vivianite was identified by XRD also after the re-aeration treatment; however, the peaks appeared smaller than in the samples before aeration (Figure 2).

4 Discussion

4.1 Sink-switch from redox-sensitive to redox-stable Fe-bound P under anoxic conditions

4.1.1 Solid phase transformation

Sink-switching from redox-sensitive Fe(III)-P to redox-stable Fe(II)-P, often identified as vivianite, has been observed in laboratory experiments (Berg et al. 2020; Borch et al. 2007; Hansen and Poulsen 1999) and in field studies of limnic (Manning et al. 1991; Markovic et al. 2019; Rothe et al. 2014; Vuillemin et al. 2020), and marine systems (Egger et al. 2015; Liu et al.

2018). Through an experimental approach we showed that redox-sensitive P adsorbed to amorphous $Fe(OH)_3$ was transformed to redox-stable Fe-bound P (Figure 1) under anoxic conditions in two different lake sediments (Table 1). Overall, approximately 70 % of the initially added Fe-bound P was immobilized during the anoxic conditions. As the redox-sensitive Fe and P decreased to the same extent, they were converted together. The determination of P binding forms by sequential extraction showed noticeable standard and systematic deviations between non-parallel fractionations (Figure 1). The deviations displayed in our data are in the range of common yield gaps and errors of sequential P extraction (Ribeiro et al. 2008; Rothe et al. 2015).

A previous study has shown that the redox-stable NaOH-SRP fraction extracts the major part of synthetic vivianite (Rothe et al. 2015). Our analyses support this observation since the formation of redox-stable Fe-bound P (NaOH-SRP) came along with the formation of vivianite (Figure 2). The quantitative estimations of the mineral by sequential extraction and XRD resulted in well comparable values within the same order of magnitude. Namely, vivianite quantified by XRD yielded 87 % of the NaOH-SRP fraction for the Müggelsee sediment and 142 % for the sediment from Langer See (see chapter 3.2). On the one hand, this substantiates the NaOH-SRP fraction of the applied extraction scheme as an indicator for vivianite in Fe-dominated systems. On the other hand, this finding suggests that most or all P extracted as NaOH-SRP was vivianite.

4.1.2 Physicochemical conditions during anoxic Fe-P sink-switching

The higher values of pore water pH in the $Fe(OH)_3$-P amended sediments during anoxic incubation (Table 3), were consistent with the presumption that in these batches the release of OH^- was higher because of the more intensive reduction of amorphous $Fe(OH)_3$. It was found

that pH 6.0 – 9.0 was optimal for the formation of vivianite (Cao et al. 2019) and the mineral was stable in this pH range (Rothe et al. 2016). Room temperature (in our study 27 ± 2 °C) provides conditions conducive to vivianite precipitation (Madsen and Hansen 2014), and the redox potential (Table 3) was low enough for $Fe(OH)_3$ reduction (Glasauer et al. 2003; Lindsay 1979). The molar Fe/P ratio in the redox-sensitive fraction (Table 2) at the start of anoxic incubation was close to the stoichiometric Fe/P-ratio of vivianite (i.e. 1.5). Furthermore, because of the surplus Fe, the treated sediments were non-sulphidic (Berner 1981; Rothe et al. 2016) as the sedimentary S/Fe-ratios were below 1.1 (Table 1) and sulphate reduction was limited to the initial sulphate supply in the overlying water of the closed experimental system. Therefore, the physicochemical conditions in our study were conducive to vivianite formation.

4.1.3 Microbial community alteration during anoxic Fe-P sink-switching

OTUs of classified genera, which accounted for the significant dissimilarity of the bacterial community composition in the sediments from Müggelsee with time (PERMANOVA: $p = 0.001$), are indicators for the redox conditions in the sediment because of their metabolic characteristics. The abundance of OTUs with high homology to the aerobic genera *Ilumatobacter* sp. and *Gaiella* sp., (Albuquerque et al. 2011; Matsumoto et al. 2009) decreased during anoxic incubation, whereas the abundance of OTUs affiliated to the anaerobic *Ignavibacterium* sp. and *Hydrogenispora* sp. (Iino et al. 2010; Liu et al. 2014) increased. This substantiates that the redox potential in the Müggelsee sediment was higher before incubation (aerobic) and the bacterial community composition changed because of anoxic incubation. After 13 anoxic days, no significant difference was observed in the community composition between the naturally Fe-rich controls, without observed vivianite formation, and the treatments with

extra Fe and P, with vivianite having formed (PERMANOVA: $p = 0.09$). On the one hand, these data showed that the surplus Fe and P in the sediment solids did not significantly affect the microbial community composition. On the other hand, the bacterial community composition, along with measurable vivianite formation of the treated sediments, was not distinct from the control sediment population.

In the naturally Fe-poor sediment from Langer See, the manipulation by the addition of $Fe(OH)_3$-P caused a highly significant dissimilarity in the bacterial community composition in comparison with that of the control sediments (PERMANOVA: $p = 0.001$). This suggested that the microbial community composition changed instantly (i.e. within a few hours between the preparation of the treated and the control sediments and freezing them) because of the surplus Fe and P in the sediment solids. Similarly, an immediate start of Fe(III)-reduction has been observed by Rasmussen and Nielsen (1996) and by Wang et al. (2019) after activated sludge had been exposed to anaerobic conditions. In the sediments from Langer See, the abundances of *Ilumatobacter* sp. and *Cyanobium* sp. increased in the treated sediments in comparison to the control samples, but these genera were not related to direct Fe-reduction (Melton et al. 2014; Weber et al. 2006). However, the great amount of OTUs affiliated to unclassified genera did not allow a conclusion on whether the observed Fe-reduction was directly microbial mediated. These data also indicated the need for further research on the classification of microbial communities in lake sediments, as well as investigations uncovering the metabolic pathways of the sediment inhabiting bacterial populations. Hypothetically, members of *β*- and *γ*-*Proteobacteria* contributed to the Fe-reduction in the treatments from Langer See because OTUs assigned to these classes were more abundant in the treated than in the control

sediments and these classes contain various Fe-reducing species (Weber et al. 2006). Further, the composition of the bacterial communities inhabiting the treated sediments from Langer See changed significantly over time (PERMANOVA: $p = 0.03$). The OTU affiliated to *Thiobacillus* sp., which has been shown to reduce Fe (Suzuki et al. 1990), might have reduced Fe in the treated sediments from Langer See, as its abundance within these samples increased with time.

Vivianite formation from redox-sensitive Fe and P could be microbially controlled by Fe-reduction. In batch culture experiments and sewage digestion, well-known direct Fe-reducers, such as *Geobacter* spp., *Shewanella* spp*., Dechloromonas* spp., and *Clostridiaceae* have been observed to mediate vivianite formation by Fe-reduction (Cao et al. 2019; Glasauer et al. 2003; Wang et al. 2019; Wang et al. 2018). Comensoli et al. (2017) observed higher bacterial than abiotic Fe-reduction efficiencies resulting in higher amounts of vivianite formation on a corroded Fe(III)-surface. Ionescu et al. (2015) stated that the differentiation between Fe-reduction as a direct metabolic or abiotic process might not be the question, as abiotic Fe-reduction is also mediated by substrates of biological origin. This factor makes the group of bacteria indirectly involved in the process of vivianite formation even larger than only the bacteria capable of direct Fe-reduction. Despite, this study did not identify known direct Fe-reducers assisting vivianite formation, Fe-reduction clearly depends on microbial activity in natural systems such as lake sediments.

In addition, bacteria could mediate the precipitation of the mineral. Sanchez-Roman et al. (2015) found microbially mediated precipitation of vivianite, as vivianite formation occurred only in cultures with active cells of *Tessarococcus lapidicaptus* and not in anaerobic sterile

controls despite vivianite supersaturation. However, vivianite precipitation has been observed to occur also abiotically (Berg et al. 2020; Borch et al. 2007).

In summary, microbial activity is not mandatory for vivianite formation but can enable and enhance the process in natural environments. Under laboratory conditions, the microbial communities of two lake sediments adapted to anoxic conditions and to the presence of Fe(III) as electron acceptor within the time frame of vivianite formation and, therefore, mediated the formation of the mineral by indirect or direct Fe-reduction.

4.2 Fe-hydroxide with adsorbed P acts as a precursor for vivianite

4.2.1 Role of pore water supersaturation

Saturation indices are common thermodynamic tools to predict the precipitation and dissolution of mineral phases in water. In the incubated sediments, except one from Fe-poor Langer See without the addition of $Fe(OH)_3$-P, vivianite was supersaturated but its formation was observed only in the sediments with initial $Fe(OH)_3$-P addition. Therefore, $Fe(OH)_3$-P acted as a precursor of vivianite. Despite its supersaturation, vivianite formation was not measurable in the control sediment from Müggelsee during anoxic incubation. Boers and de Bles (1991), as well as Davison (1993), conclude that pore water supersaturation is not conclusive evidence of mineral presence because of kinetic hindrance, competing reactions, and failure to analyse the actually reacting species. Also small-scale heterogeneity within the sediment matrix has been considered to explain why pore water supersaturation of vivianite has often been reported to fail in predicting the minerals occurrence (Glasauer et al. 2003; Rothe et al. 2016). A solid precursor containing Fe and P likely generates microzones where the precipitation of the

466 mineral is favoured. Vivianite precipitation could occur close to the precursor (Nanzyo et al.
467 2013) within a steep pore water gradient of dissolved Fe(II) and P or directly on the surface of
468 the precursor (Vuillemin et al. 2020).

469 **4.2.2 Vivianite precursors and their occurrence**

470 In addition to P adsorbed to $Fe(OH)_3$, other ferric Fe(oxy-hydr)oxides with adsorbed P have
471 been suggested as precursors of vivianite (Egger et al. 2015; Hearn et al. 1983; Liu et al. 2018;
472 Rothe et al. 2016; Vuillemin et al. 2020). Further, vivianite formation has been attributed
473 conclusively to precursors such as P adsorbed on hydrated ferric oxide (Manning et al. 1991),
474 ferrihydrite with adsorbed P (Borch et al. 2007), amorphous Fe(III)-phosphate (Berg et al. 2020),
475 and green rust phases with sorbed P (Hansen and Poulsen 1999).

476 These P binding Fe(III) or mixed valence Fe minerals typically occur at the oxic-anoxic
477 water-sediment interface of Fe-rich and S-poor lakes (Berner 1981; Vuillemin et al. 2020). In
478 particular in shallow lake sediments, oxic and anoxic periods often follow one after another.
479 Thus, sorption of P to Fe(oxy-hydr)oxides and re-dissolution of these compounds occur regularly
480 (Parsons et al. 2017). These redox shifts provide the conditions for vivianite formation from
481 redox-sensitive Fe-P precursors.

482 Vivianite precurors are also present in marine systems and waterlogged soils. In the oceans, P
483 is bound to Fe(oxy-hydr)oxides precipitating in the oxic water column and afterwards depositing
484 in the sediment (März et al. 2008). Redoximorphic soils contain poorly crystalline Fe-oxide
485 concretions with high P contents (Gasparatos et al. 2019). Vivianite precursors may also form in
486 soils which are percolated by P-rich solutions, e.g. originating from P fertilisers (Kusunoki et al.

2015), and containing Fe(III)-phases (Hansen and Poulsen 1999). Furthermore, vivianite formation has been attributed to separate sources of Fe and P, usually with Fe originating from the catchment and P from organic matter (Dijkstra et al. 2016; Grizelj et al. 2017; Vuillemin et al. 2013). It can only be hypothesised whether in these environments redox-sensitive Fe(III)-P precursors form before vivianite precipitation.

4.3 Implications for P management

4.3.1 Time frame of P immobilisation and effect on pore water P

In our study, the sink-switch from redox-sensitive to redox-stable P occurred mostly during the first 40 d and was fastest at the beginning of the anoxic incubation. This time frame for vivianite formation from Fe(III) bound P conforms with the findings of other studies in bacterial inoculated soil slurries (Borch and Fendorf 2007) and digested sewage sludge (Wang et al. 2019). Further, vivianite occurrence was observed within seasonal flooding lasting a few months in paddy fields (Kusunoki et al. 2015) and ascribed to summer periods in a varved sediment (Zarczynski et al. 2019). Redox conditions change regularly in the surface sediments of shallow lakes; therefore, anoxic conditions caused by stratification periods could be crucial for P immobilisation through sink-switch from redox-sensitive to redox-stable Fe-P phases, such as vivianite.

Vivianite formation has been termed as 'slow' (Madsen and Hansen 2014; Walpersdorf et al. 2013), as the process does not control the pore water chemistry of P (Emerson and Widmer 1978). In fact, in our experiments, despite ongoing vivianite precipitation, the saturation index did not reach equilibrium (Table 3). However, lower pore water P in the treated sediments did

indicate less P mobilisation in comparison with the control sediments (Figure 3). The inhibition of P release from sediments after treatment with Fe (Chen et al. 2016; Fuchs et al. 2018; Orihel et al. 2016) demonstrates that Fe precipitation of P is effective also during anoxic periods.

4.3.2 Reversibility of Fe-P sink-switch after oxygenation

Dynamic redox conditions in shallow water bodies can be ascribed to bioturbation, root activity, sediment resuspension, and seasonal O_2 fluctuation (Parsons et al. 2017). Therefore, re-oxygenation of the sediment could occur after the anoxic immobilisation of Fe-bound P as vivianite. Discussions have been conducted on whether vivianite is transformed under oxidising conditions. In contact with air, 50 % of Fe in vivianite is oxidised at room temperature (Rouzies and Millet 1993) and further oxidation occurs at higher temperatures (Rothe et al. 2016). After draining previously flooded rice fields, the vivianite content attached to rice roots was shown to decrease because of re-oxygenation (Kusunoki et al. 2015). In batch culture experiments, suspended vivianite was transformed through an amorphous mixed valence Fe-P compound to Fe(III)-P (Miot et al. 2009). As no transformation occurred in the absence of dissolved Fe(II) and in sterile controls, it was suggested that vivianite was oxidised by the by-product nitrite (Miot et al. 2009). Vivianite oxidation has been suggested also in sediments in-situ (Liu et al. 2018). In our experiments, the short but thorough re-oxygenation of the sediments did oxidise Fe compounds according to the increase in BD-Fe. However, the freshly formed redox-stable P remained in this fraction and did not relocate to the redox-sensitive Fe, although, according to XRD analyses, vivianite could have been altered partly. Overall, this indicated that the immobilisation of anoxic conditions was not reversed.

4.3.3 Controlling P immobilisation by Fe under anoxic conditions in lake sediments

The immobilisation of P and inhibition of P release from sediments imply that P management by relying on Fe is promising under anoxic conditions. The question is how to induce this process.

The redox-sensitive Fe-P compounds identified as precursors of this sink-switch occur at oxic sediment surfaces. Therefore, in Fe-rich lakes, the artificial or natural oxygenation of the upper sediment layers through bioturbation or around submerged macrophyte roots (Hupfer and Dollan 2003) promotes the occurrence of the precursors. In particular, at the topmost sediment layers and because of the activity of chironomids (Hupfer et al. 2019), low molar Fe/P ratios are observed in the redox-sensitive fraction, similar to the precursor applied in this study. After the onset of anoxic conditions at the sediment water interface because of stratification of the water column, the termination of bioturbation or after burial to deeper anoxic sediment layers, the precursors can be transformed and increase long-term P burial.

However, the formation of vivianite competes with other Fe(II)-minerals such as siderite (Vuillemin et al. 2020) and Fe-sulphides (Gächter and Müller 2003; Rothe et al. 2015). If the ligands competing with P are limited, Fe dosing is an obvious management measure to provide excess Fe (Kleeberg et al. 2013) to form the precursor of redox-stable Fe-bound P. Fe amendments are logistically and financially feasible in most freshwater lakes (Orihel et al. 2016).

5 Conclusions

- The redox cycling of Fe in freshwater sediments plays an important role not only in temporary P binding by ferric Fe but, particularly, for long-term storage of P coupled to ferrous Fe.
- The immobilisation of P by Fe under anoxic non-sulphidogenic conditions occurs by the formation of the reduced Fe(II)-P mineral vivianite.
- The presence of Fe-(hydr)oxides with adsorbed P is a controlling factor for the formation of vivianite and it acts as a precursor. In contrast, pore water supersaturation is not a good indicator for vivianite formation.
- The sink-switch and formation of vivianite are feasible within 40 d under laboratory conditions, which is a relevant time scale of anoxic periods in natural systems. Within this time frame also the microbial communities, mediating the process, adapt to changing conditions either from oxic to anoxic as well as to the presence of Fe(III) as electron acceptor. Even after re-oxygenation, the vivianite phase remains redox-stable.
- Fe dosing as a management measure for long-term immobilisation of P in the sediments of eutrophic lakes is promising, even if anoxic periods occur. As vivianite precursors, redox-sensitive Fe-P compounds occur at oxic sediment surfaces in Fe-rich lakes. The oxygenation of upper sediment layers promotes the occurrence of the precursors. In relatively Fe-poor lakes, Fe dosing yielding a molar BD-Fe/BD-TP ratio of 1.5 can provide excess Fe to form the precursors.

Acknowledgements

This work was funded by the German Research Foundation (DFG) as part of the Research Training Group ''Urban Water Interfaces (UWI)'' (GRK 2032/2, Project F3: ''Controlling of phosphorus fluxes in urban systems: Analogous processes in limnic sediments and sewage sludges''). The Department of Environmental Microbiology (TU Berlin) offered their facilities and assistance in DNA extraction for the analysis of the microbial community composition (T. Fritscher-Klöppel). If not stated otherwise, the XRD analyses were conducted at the Department of Inorganic Chemistry (TU Berlin, I. Speckman). We are grateful to the Department of Chemical Analytics and Biogeochemistry of IGB Berlin for assistance with chemical analyses, discussions on the experimental set-up, and the results, and for financing of the bacterial 16S rRNA gene amplicon sequencing and of the vivianite quantification by XRD carried out at Landeslabor Berlin-Brandenburg. We would like to thank Editage (www.editage.com) for English language editing.

Literature

Albuquerque, L., Franca, L., Rainey, F.A., Schumann, P., Nobre, M.F. and da Costa, M.S., 2011. Gaiella occulta gen. nov., sp. nov., a novel representative of a deep branching phylogenetic lineage within the class Actinobacteria and proposal of Gaiellaceae fam. nov. and Gaiellales ord. nov. Systematic and Applied Microbiology 34(8), 595-599.

Altomare, A., Corriero, N., Cuocci, C., Falcicchio, A., Moliterni, A. and Rizzi, R., 2015. QUALX2.0: a qualitative phase analysis software using the freely available database POW_COD. Journal of Applied Crystallography 48(2), 598-603.

Berg, J.S., Duverger, A., Cordier, L., Laberty-Robert, C., Guyot, F. and Miot, J., 2020. Rapid pyritization in the presence of a sulfur/sulfate-reducing bacterial consortium. Scientific Reports 10(1), 8264.

Berner, R.A., 1981. A new geochemical classification of sedimentary environments. Journal of Sedimentary Research 51(2), 359-365.

Boers, P. and de Bles, F., 1991. Ion concentrations in interstitial water as indicators for phosphorus release processes and reactions. Water Research 25(5), 591-598.

Borch, T. and Fendorf, S., 2007. Chapter 12 Phosphate Interactions with Iron (Hydr)oxides: Mineralization Pathways and Phosphorus Retention upon Bioreduction, Elsevier.

Borch, T., Masue, Y., Kukkadapu, R.K. and Fendorf, S., 2007. Phosphate imposed limitations on biological reduction and alteration of ferrihydrite. Environmental Science & Technology 41(1), 166-172.

Cao, J., Wu, Y., Zhao, J., Jin, S., Aleem, M., Zhang, Q., Fang, F., Xue, Z. and Luo, J., 2019. Phosphorus recovery as vivianite from waste activated sludge via optimizing iron source and pH value during anaerobic fermentation. Bioresource Technology 293, 122088.

Chen, M., Sun, H.Q. and Jiang, H.L., 2016. The addition of FeOOH binds phosphate in organic matter-rich sediments. Chemistry and Ecology 32(5), 432-445.

Comensoli, L., Maillard, J., Albini, M., Sandoz, F., Junier, P. and Joseph, E., 2017. Use of Bacteria To Stabilize Archaeological Iron. Applied and Environmental Microbiology 83(9), 83:e03478-03416. .

Cooke, G.D., Welch, E.B., Martin, A.B., Fulmer, D.G., Hyde, J.B. and Schrieve, G.D., 1993. Effectiveness of Al, Ca, and Fe salts for control of internal phosphorus loading in shallow and deep lakes. Hydrobiologia 253(1), 323-335.

Davison, W., 1993. Iron and manganese in lakes. Earth-Science Reviews 34(2), 119-163.

Dijkstra, N., Slomp, C.P., Behrends, T. and Expedition 347 Scientists, 2016. Vivianite is a key sink for phosphorus in sediments of the Landsort Deep, an intermittently anoxic deep basin in the Baltic Sea. Chemical Geology 438, 58-72.

Egger, M., Jilbert, T., Behrends, T., Rivard, C. and Slomp, C.P., 2015. Vivianite is a major sink for phosphorus in methanogenic coastal surface sediments. Geochimica Et Cosmochimica Acta 169, 217-235.

Emerson, S. and Widmer, G., 1978. Early diagenesis in anaerobic lake sediments—II. Thermodynamic and kinetic factors controlling the formation of iron phosphate. Geochimica Et Cosmochimica Acta 42(9), 1307-1316.

Frossard, E., Bauer, J.P. and Lothe, F., 1997. Evidence of vivianite in FeSO4-flocculated sludges. Water Research 31(10), 2449-2454.

Fuchs, E., Funes, A., Saar, K., Reitzel, K. and Jensen, H.S., 2018. Evaluation of dried amorphous ferric hydroxide CFH-12 (R) as agent for binding bioavailable phosphorus in lake sediments. Science of The Total Environment 628-629, 990-996.

Gächter, R. and Müller, B., 2003. Why the phosphorus retention of lakes does not necessarily depend on the oxygen supply to their sediment surface. Limnology and Oceanography 48(2), 929-933.

Gasparatos, D., Massas, I. and Godelitsas, A., 2019. Fe-Mn concretions and nodules formation in redoximorphic soils and their role on soil phosphorus dynamics: Current knowledge and gaps. Catena 182, 104106.
Glasauer, S., Weidler, P.G., Langley, S. and Beveridge, T.J., 2003. Controls on Fe reduction and mineral formation by a subsurface bacterium. Geochimica Et Cosmochimica Acta 67(7), 1277-1288.
Grazulis, S., Chateigner, D., Downs, R.T., Yokochi, A.F., Quiros, M., Lutterotti, L., Manakova, E., Butkus, J., Moeck, P. and Le Bail, A., 2009. Crystallography Open Database - an open-access collection of crystal structures. Journal of Applied Crystallography 42(Pt 4), 726-729.
Grizelj, A., Bakrac, K., Horvat, M., Avanic, R. and Hecimovic, I., 2017. Occurrence of vivianite in alluvial Quaternary sediments in the area of Sesvete (Zagreb, Croatia). Geologia Croatica 70(1), 41-52.
Habraken, W.J.E.M., Tao, J., Brylka, L.J., Friedrich, H., Bertinetti, L., Schenk, A.S., Verch, A., Dmitrovic, V., Bomans, P.H.H., Frederik, P.M., Laven, J., van der Schoot, P., Aichmayer, B., de With, G., DeYoreo, J.J. and Sommerdijk, N.A.J.M., 2013. Ion-association complexes unite classical and non-classical theories for the biomimetic nucleation of calcium phosphate. Nature Communications 4(1), 1507.
Hansen, H.C.B. and Poulsen, I.F., 1999. Interaction of Synthetic Sulphate "Green Rust" with Phosphate and the Crystallization of Vivianite. Clays and Clay Minerals 47(3), 312-318.
Hearn, P.P., Parkhurst, D.L. and Callender, E., 1983. Authigenic Vivianite in Potomac River Sediments: Control by Ferric Oxy-Hydroxides. Journal of Sedimentary Research 53(1), 165-177.
Hupfer, M. and Dollan, A., 2003. Immobilisation of phosphorus by iron-coated roots of submerged macrophytes. Hydrobiologia 506(1), 635-640.
Hupfer, M., Gächter, R. and Giovanoli, R., 1995. Transformation of phosphorus species in settling seston and during early sediment diagenesis. Aquatic Sciences 57(4), 305-324.
Hupfer, M., Jordan, S., Herzog, C., Ebeling, C., Ladwig, R., Rothe, M. and Lewandowski, J., 2019. Chironomid larvae enhance phosphorus burial in lake sediments: Insights from long-term and short-term experiments. Science of The Total Environment 663, 254-264.
Iino, T., Mori, K., Uchino, Y., Nakagawa, T., Harayama, S. and Suzuki, K., 2010. Ignavibacterium album gen. nov., sp. nov., a moderately thermophilic anaerobic bacterium isolated from microbial mats at a terrestrial hot spring and proposal of Ignavibacteria classis nov., for a novel lineage at the periphery of green sulfur bacteria. International Journal of Systematic and Evolutionary Microbiology 60(Pt 6), 1376-1382.
Ionescu, D., Heim, C., Polerecky, L., Thiel, V. and de Beer, D., 2015. Biotic and abiotic oxidation and reduction of iron at circumneutral pH are inseparable processes under natural conditions. Geomicrobiology Journal 32(3-4), 221-230.
Kleeberg, A., Herzog, C. and Hupfer, M., 2013. Redox sensitivity of iron in phosphorus binding does not impede lake restoration. Water Research 47(3), 1491-1502.
Kusunoki, A., Nanzyo, M., Kanno, H. and Takahashi, T., 2015. Effect of water management on the vivianite content of paddy-rice roots. Soil Science and Plant Nutrition 61(6), 910-916.
Lindsay, W.L., 1979. Chemical Equilibria in Soils, Wiley-Interscience.
Liu, J.R., Izon, G., Wang, J.S., Antler, G., Wang, Z., Zhao, J. and Egger, M., 2018. Vivianite formation in methane-rich deep-sea sediments from the South China Sea. Biogeosciences 15(20), 6329-6348.
Liu, Y., Qiao, J.T., Yuan, X.Z., Guo, R.B. and Qiu, Y.L., 2014. Hydrogenispora ethanolica gen. nov., sp. nov., an anaerobic carbohydrate-fermenting bacterium from anaerobic sludge. International Journal of Systematic and Evolutionary Microbiology 64(Pt 5), 1756-1762.
Madsen, H.E.L. and Hansen, H.C.B., 2014. Kinetics of crystal growth of vivianite, Fe3(PO4)2·8H2O, from solution at 25, 35 and 45 °C. Journal of Crystal Growth 401, 82-86.
Manning, P., Tom, M. and Prepas, E., 1991. Intensive formation of vivianite in the bottom sediments of mesotrophic Narrow Lake, Alberta. The Canadian Mineralogist 29, 77-85.

673 Markovic, S., Liang, A.Q., Watson, S.B., Depew, D., Zastepa, A., Surana, P., Vanden Byllaardt, J.,
674 Arhonditsis, G. and Dittrich, M., 2019. Reduction of industrial iron pollution promotes phosphorus
675 internal loading in eutrophic Hamilton Harbour, Lake Ontario, Canada. Environmental Pollution 252,
676 697-705.
677 März, C., Poulton, S.W., Beckmann, B., Küster, K., Wagner, T. and Kasten, S., 2008. Redox sensitivity of P
678 cycling during marine black shale formation: Dynamics of sulfidic and anoxic, non-sulfidic bottom
679 waters. Geochimica Et Cosmochimica Acta 72(15), 3703-3717.
680 Matsumoto, A., Kasai, H., Matsuo, Y., Omura, S., Shizuri, Y. and Takahashi, Y., 2009. Ilumatobacter
681 fluminis gen. nov., sp. nov., a novel actinobacterium isolated from the sediment of an estuary. Journal
682 of General and Applied Microbiology 55(3), 201-205.
683 Melton, E.D., Swanner, E.D., Behrens, S., Schmidt, C. and Kappler, A., 2014. The interplay of microbially
684 mediated and abiotic reactions in the biogeochemical Fe cycle. Nature Reviews Microbiology 12(12),
685 797-808.
686 Miot, J., Benzerara, K., Morin, G., Bernard, S., Beyssac, O., Larquet, E., Kappler, A. and Guyot, F., 2009.
687 Transformation of vivianite by anaerobic nitrate-reducing iron-oxidizing bacteria. Geobiology 7(3),
688 373-384.
689 Nanzyo, M., Onodera, H., Hasegawa, E., Ito, K. and Kanno, H., 2013. Formation and Dissolution of
690 Vivianite in Paddy Field Soil. Soil Science Society of America Journal 77, 1452-1459.
691 Nriagu, J.O., 1972. Stability of vivianite and ion-pair formation in the system Fe3(PO4)2-H3PO4-H2O.
692 Geochimica Et Cosmochimica Acta 36(4), 459-470.
693 Oksanen, J., Blanchet, F.G., Kindt, R., Legendre, P., Minchin, P., O'Hara, R.B., Simpson, G., Solymos, P.,
694 Stevens, M.H.H. and Wagner, H., 2013. Vegan: Community Ecology Package. R Package Version. 2.0-
695 10. CRAN.
696 Orihel, D.M., Schindler, D.W., Ballard, N.C., Wilson, L.R. and Vinebrooke, R.D., 2016. Experimental iron
697 amendment suppresses toxic cyanobacteria in a hypereutrophic lake. Ecological Applications 26(5),
698 1517-1534.
699 Parkhurst, D.L. and Appelo, C.A.J., 2013. Description of input and examples for PHREEQC version 3—A
700 computer program for speciation, batch-reaction, one-dimensional transport, and inverse
701 geochemical calculations, U.S. Geological Survey Techniques and Methods.
702 Parsons, C.T., Rezanezhad, F., O'Connell, D.W. and Van Cappellen, P., 2017. Sediment phosphorus
703 speciation and mobility under dynamic redox conditions. Biogeosciences 14(14), 3585-3602.
704 Postma, D., 1980. Formation of siderite and vivianite and the pore-water composition of a Recent bog
705 sediment in Denmark. Chemical Geology 31, 225-244.
706 Psenner, R., Pucsko, R. and Sager, M., 1984. Fractionation of Organic and Inorganic Phosphorus
707 Compounds in Lake Sediments, An Attempt to Characterize Ecologically Important Fractions. Archiv
708 Fur Hydrobiologie 70, 111-155.
709 Rasmussen, H. and Nielsen, P.H., 1996. Iron reduction in activated sludge measured with different
710 extraction techniques. Water Research 30(3), 551-558.
711 Reed, D.C., Gustafsson, B.G. and Slomp, C.P., 2016. Shelf-to-basin iron shuttling enhances vivianite
712 formation in deep Baltic Sea sediments. Earth and Planetary Science Letters 434, 241-251.
713 Ribeiro, D.C., Martins, G., Nogueira, R., Cruz, J.V. and Brito, A.G., 2008. Phosphorus fractionation in
714 volcanic lake sediments (Azores - Portugal). Chemosphere 70(7), 1256-1263.
715 Rothe, M., Frederichs, T., Eder, M., Kleeberg, A. and Hupfer, M., 2014. Evidence for vivianite formation
716 and its contribution to long-term phosphorus retention in a recent lake sediment: a novel analytical
717 approach. Biogeosciences 11(18), 5169-5180.
718 Rothe, M., Kleeberg, A., Grüneberg, B., Friese, K., Perez-Mayo, M. and Hupfer, M., 2015. Sedimentary
719 Sulphur:Iron Ratio Indicates Vivianite Occurrence: A Study from Two Contrasting Freshwater Systems.
720 PLOS ONE 10(11), e0143737.

721 Rothe, M., Kleeberg, A. and Hupfer, M., 2016. The occurrence, identification and environmental
722 relevance of vivianite in waterlogged soils and aquatic sediments. Earth-Science Reviews 158, 51-64.
723 Rouzies, D. and Millet, J.M.M., 1993. Mössbauer study of synthetic oxidized vivianite at room
724 temperature. Hyperfine Interactions 77(1), 19-28.
725 Sanchez-Roman, M., Puente-Sanchez, F., Parro, V. and Amils, R., 2015. Nucleation of Fe-rich phosphates
726 and carbonates on microbial cells and exopolymeric substances. Frontiers in Microbiology 6, 1024.
727 Suzuki, I., Takeuchi, T.L., Yuthasastrakosol, T.D. and Oh, J.K., 1990. Ferrous Iron and Sulfur Oxidation and
728 Ferric Iron Reduction Activities of Thiobacillus ferrooxidans Are Affected by Growth on Ferrous Iron,
729 Sulfur, or a Sulfide Ore. Applied and Environmental Microbiology 56(6), 1620-1626.
730 Vuillemin, A., Ariztegui, D., De Coninck, A.S., Lücke, A., Mayr, C., Schubert, C.J. and
731 The PASADO Scientific Team, 2013. Origin and significance of diagenetic concretions in sediments of
732 Laguna Potrok Aike, southern Argentina. Journal of Paleolimnology 50(3), 275-291.
733 Vuillemin, A., Friese, A., Wirth, R., Schuessler, J.A., Schleicher, A.M., Kemnitz, H., Lücke, A., Bauer, K.W.,
734 Nomosatryo, S., von Blanckenburg, F., Simister, R., Ordoñez, L.G., Ariztegui, D., Henny, C., Russell,
735 J.M., Bijaksana, S., Vogel, H., Crowe, S.A. and Kallmeyer, J., 2020. Vivianite formation in ferruginous
736 sediments from Lake Towuti, Indonesia. Biogeosciences 17(7), 1955-1973.
737 Walpersdorf, E., Koch, C.B., Heiberg, L., O'Connell, D.W., Kjaergaard, C. and Hansen, H.C.B., 2013. Does
738 vivianite control phosphate solubility in anoxic meadow soils? Geoderma 193-194, 189-199.
739 Wang, R., Wilfert, P., Dugulan, I., Goubitz, K., Korving, L., Witkamp, G.-J. and van Loosdrecht, M.C.M.,
740 2019. Fe(III) reduction and vivianite formation in activated sludge. Separation and Purification
741 Technology 220, 126-135.
742 Wang, S., An, J.K., Wan, Y.X., Du, Q., Wang, X., Cheng, X. and Li, N., 2018. Phosphorus Competition in
743 Bioinduced Vivianite Recovery from Wastewater. Environmental Science & Technology 52(23), 13863-
744 13870.
745 Weber, K.A., Achenbach, L.A. and Coates, J.D., 2006. Microorganisms pumping iron: anaerobic microbial
746 iron oxidation and reduction. Nature Reviews Microbiology 4(10), 752-764.
747 Wilfert, P., Dugulan, A.I., Goubitz, K., Korving, L., Witkamp, G.J. and Van Loosdrecht, M.C.M., 2018.
748 Vivianite as the main phosphate mineral in digested sewage sludge and its role for phosphate
749 recovery. Water Research 144, 312-321.
750 Wilfert, P., Mandalidis, A., Dugulan, A.I., Goubitz, K., Korving, L., Temmink, H., Witkamp, G.J. and Van
751 Loosdrecht, M.C.M., 2016. Vivianite as an important iron phosphate precipitate in sewage treatment
752 plants. Water Research 104, 449-460.
753 Zarczynski, M., Wacnik, A. and Tylmann, W., 2019. Tracing lake mixing and oxygenation regime using the
754 Fe/Mn ratio in varved sediments: 2000 year-long record of human-induced changes from Lake
755 Zabinskie (NE Poland). Science of The Total Environment 657, 585-596.
756 Zhang, X., 2012. Factors Influencing Iron Reduction–Induced Phosphorus Precipitation. Environmental
757 Engineering Science 29(6), 511-519.
758

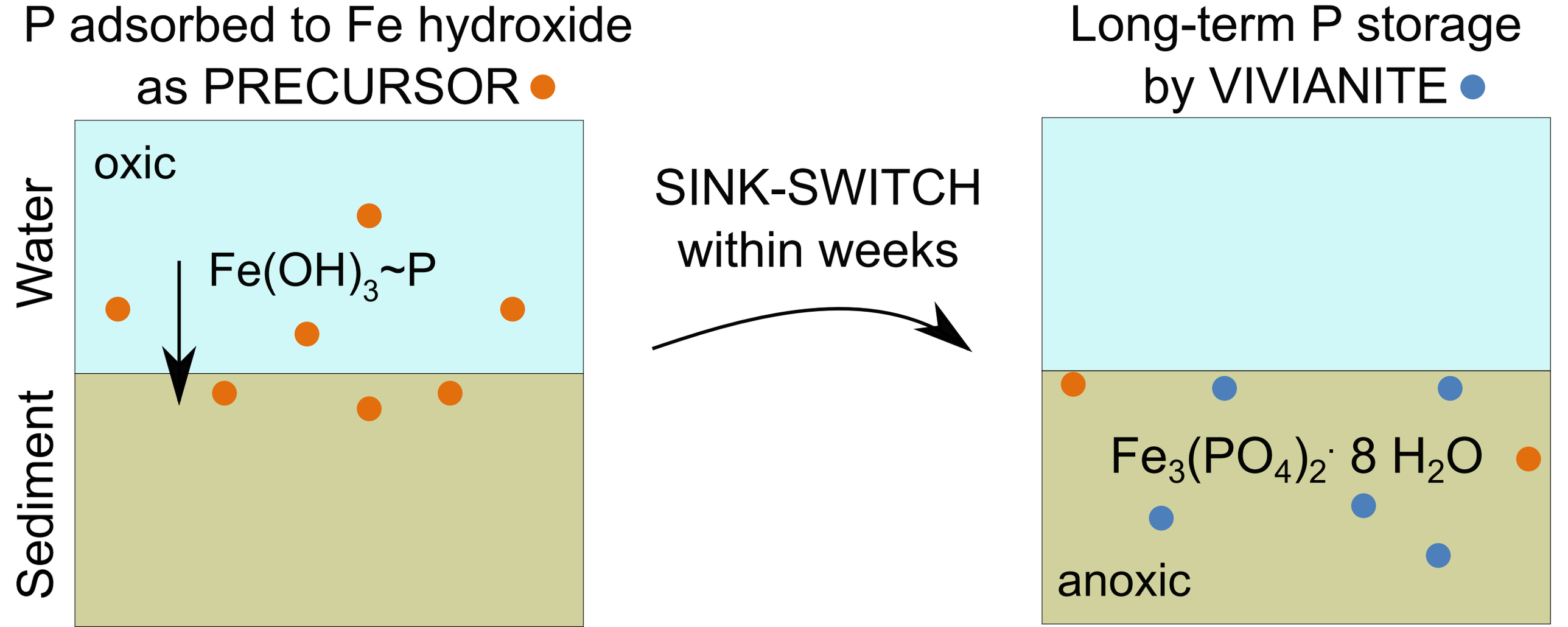
P adsorbed to Fe hydroxide
as PRECURSOR
Water
Sediment
oxic
Fe(OH)3~P
SINK-SWITCH
within weeks
Long-term P storage
by VIVIANITE
Fe3(PO4)2· 8 H2O
anoxic

Highlights

- Vivianite formed in lake sediments during oxic-anoxic sink-switch within 40 d.
- P adsorbed to Fe(III)hydroxide as precursor was vital to vivianite formation.
- Microbial communities adapted to anoxic condition and Fe(III) as electron acceptor.
- Vivianite P did not retransfer to a redox-sensitive P binding form under oxic state.
- Fe amendments are promising for long-term P immobilisation in lake sediment.

Table 1
Click here to download Table: Table1.docx

Table 1 Physicochemical differentiation of the control and the extra $Fe(OH)_3$-P-containing sediments from Müggelsee and Langer See (N = 4): molar Fe, P, and S contents, molar S/Fe and Fe/P ratios, dry weight (DW), and organic matter (OM) content determined as of loss on ignition (450 °C). Significant differences ($p \leq 0.05$) between the controls and treatments are indicated by asterisks (*).

	Fe µmol/g DW	P µmol/g DW	S µmol/g DW	S/Fe	Fe/P	DW %	OM %
Müggelsee Fe-P	769 ± 19 *	225 ± 5 *	313 ± 7	0.41 ± 0.01 *	3.42 ± 0.09 *	20 ± 1	19 ± 1
Müggelsee Control	559 ± 15	100 ± 7	321 ± 11	0.57 ± 0.01	5.58 ± 0.32	19 ± 1	19 ± 1
Langer See Fe-P	631 ± 8 *	319 ± 2 *	476 ± 7 *	0.75 ± 0.01 *	1.98 ± 0.02 *	10 ± 1	23 ± 1 *
Langer See Control	219 ± 4	62 ± 9	508 ± 13	2.32 ± 0.02	3.63 ± 0.50	10 ± 1	24 ± 1

Table 2
Click here to download Table: Table2.docx

Table 2 Molar BD-Fe/BD-TP ratios at the start and end of anoxic incubation and after the re-aeration of the control and treated sediments with initial addition of $Fe(OH)_3$-P from Müggelsee and Langer See (N = 4). Significant differences ($p \leq 0.05$) in comparison to the previous experimental step (1, 2, and 3) are indicated by asterisks (*).

	Molar BD-Fe/BD-TP ratio			
	Müggelsee Fe-P	**Müggelsee Control**	**Langer See Fe-P**	**Langer See Control**
1) Start	1.61 ± 0.05	2.18 ± 0.14	1.53 ± 0.02	2.65 ± 0.11
2) Anoxic	1.55 ± 0.04	2.19 ± 0.07	1.64 ± 0.12	2.22 ± 0.26
3) Re-aerated	2.30 ± 0.07 *	3.70 ± 0.10 *	2.12 ± 0.15 *	1.91 ± 0.22

Table 3
Click here to download Table: Table3.docx

Table 3 Pore water conditions (pH and redox potential Eh) and saturation index (SI) of the Fe(II)-P mineral vivianite, calculated after Habraken et al. (2013) and Rothe et al. (2016), in the pore water of the sediments during anoxic incubation with and without initial addition of $Fe(OH)_3$-P in contrast with actual vivianite formation (N = 24).

	pH	Eh mV	SI vivianite during anoxic incubation	Vivianite formed
Müggelsee Fe-P	7.9 ± 0.1	- 67 ± 20	1.05 ± 0.05	✓
Müggelsee Control	7.5 ± 0.1	- 35 ± 18	1.11 ± 0.03	-
Langer See Fe-P	8.0 ± 0.1	- 77 ± 10	0.81 ± 0.08	✓
Langer See Control	7.4 ± 0.1	- 182 ± 12	- 0.06 ± 0.07	-

Table 4
Click here to download Table: Table4.docx

Table 4 Estimated bacterial alpha-diversity indices, Chao1 and Simpson, before and during anoxic incubation of control and Fe-P amended sediments from Müggelsee and Langer See (N = 4). Significant differences ($p \leq 0.05$) in Chao 1 between the time steps are indicated by asterisks (*).

	Time step	Chao1		Simpson
Müggelsee Fe-P	Before incubation	332 ± 7	*	0.96
	Anoxic (13 d)	426 ± 8		0.98
Müggelsee Control	Before incubation	352 ± 13	*	0.96
	Anoxic (13 d)	414 ± 19		0.98
Langer See Fe-P	Before incubation	439 ± 8		0.97
	Anoxic (8 d)	452 ± 7		0.98
Langer See Control	Before incubation	444 ± 6		0.99
	Anoxic (8 d)	446 ± 4		0.99

Figure 1

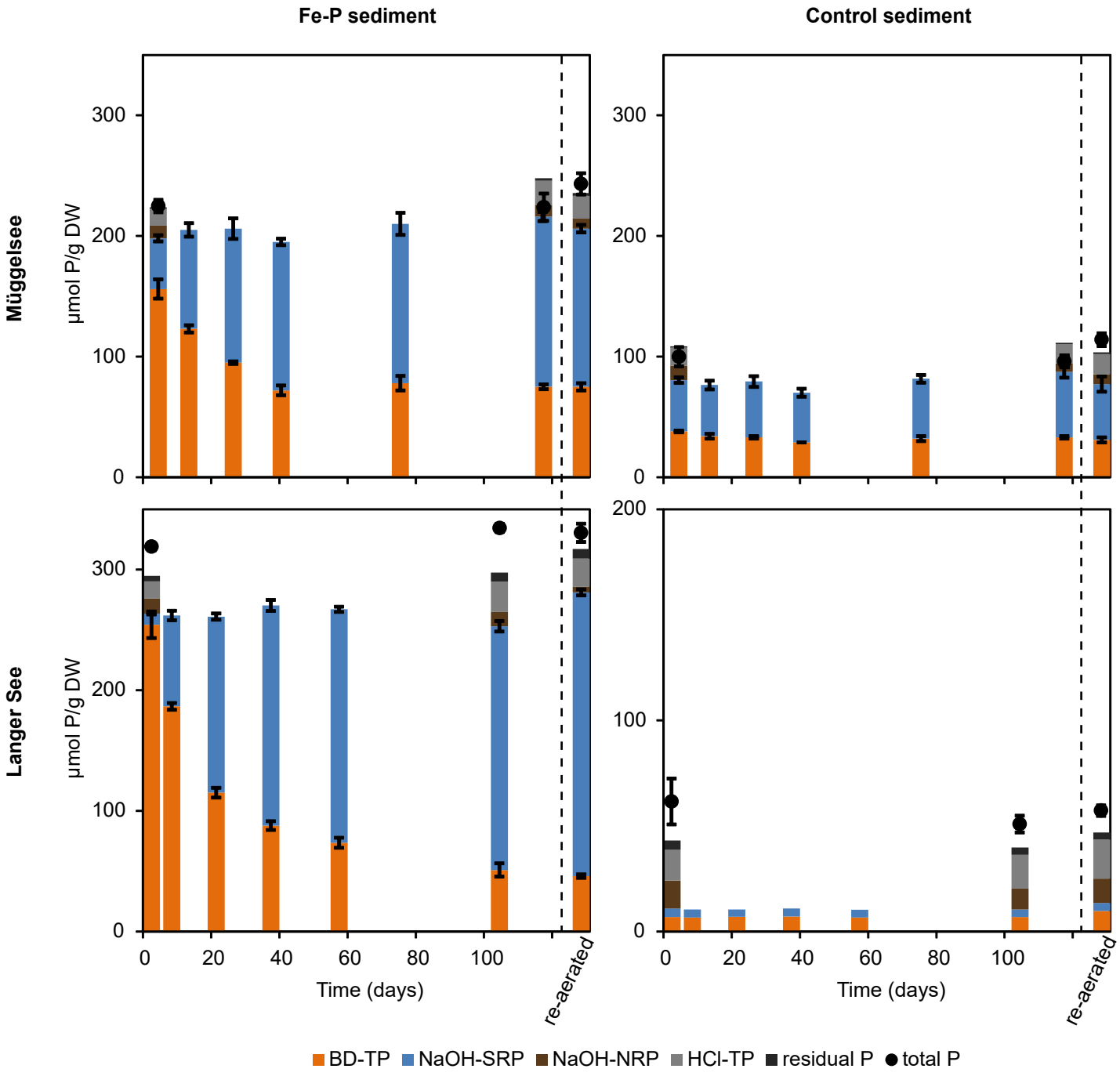

Figure 1 P-binding forms (BD-TP: redox-sensitive P; NaOH-SRP: redox-stable metal-bound P; NaOH-NRP: organic-bound P; HCl-TP: P bound in calcium carbonates and apatite, residual P) and total P content in the initial $Fe(OH)_3$-P amended and control sediments from Müggelsee and Langer See during anoxic incubation and after re-aeration (N = 4). Standard deviation is shown for BD-TP, NaOH-SRP, and total P. Note that owing to low values, the y-axis of the control sediment from Langer See is scaled differently and standard deviation is shown only for total P. A-TP (loosely sorbed P) was below 4 µmol/g DW and therefore omitted.

Figure 2

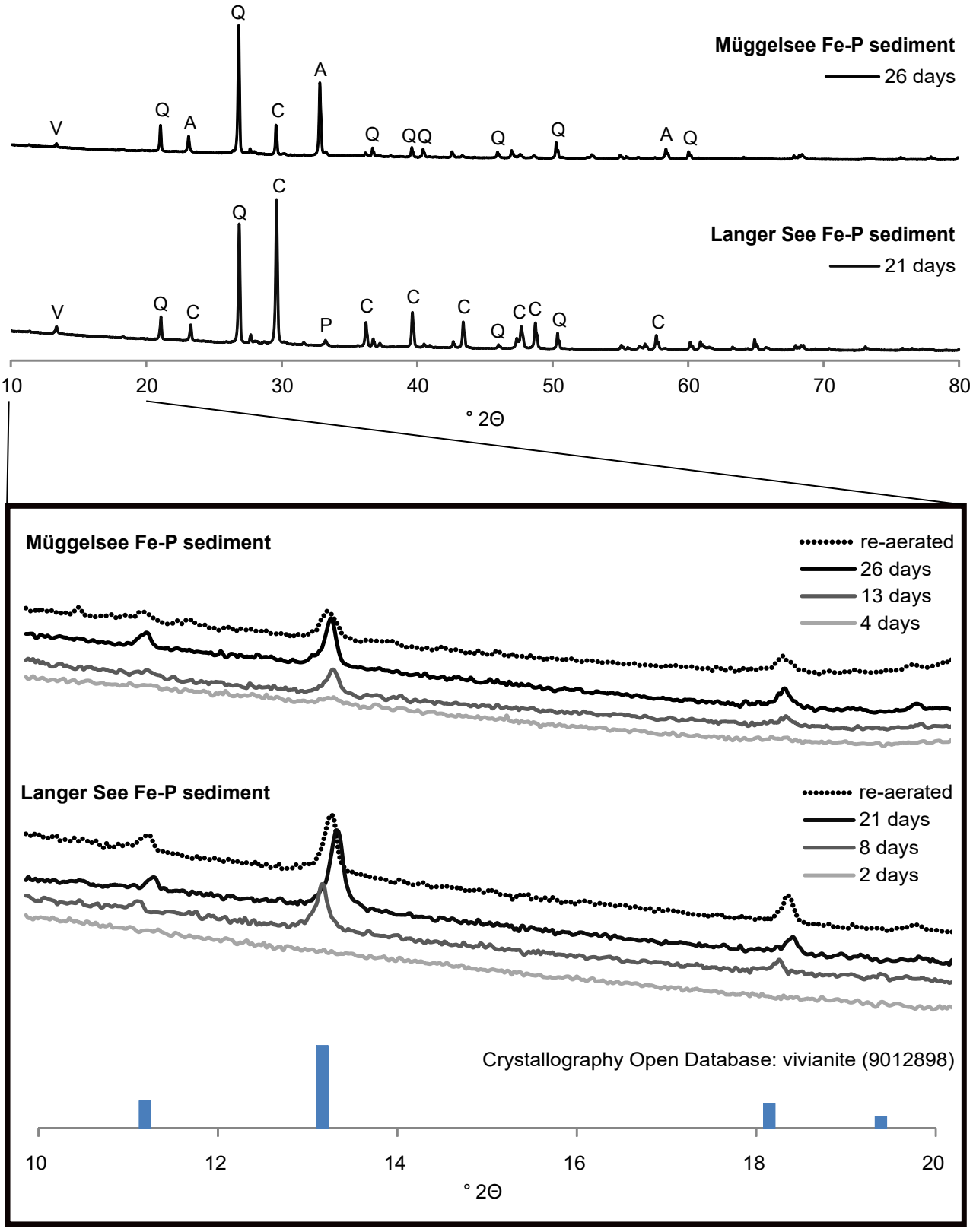

Figure 2 X-ray diffractograms of the sediments with initial addition of $Fe(OH)_3$-P. Top: broad scans of both sediments at one time step during anoxic incubation. The peaks are attributed to crystalline phases by capitals: **V**ivianite, **Q**uartz, **A**mmonium chloride, **C**alcite and **P**yrite. The box zooms in on the region where the three largest peaks of vivianite (Crystallography Open Database: 9012898) appear at three time steps of anoxic incubation and after re-aeration.

Figure 3

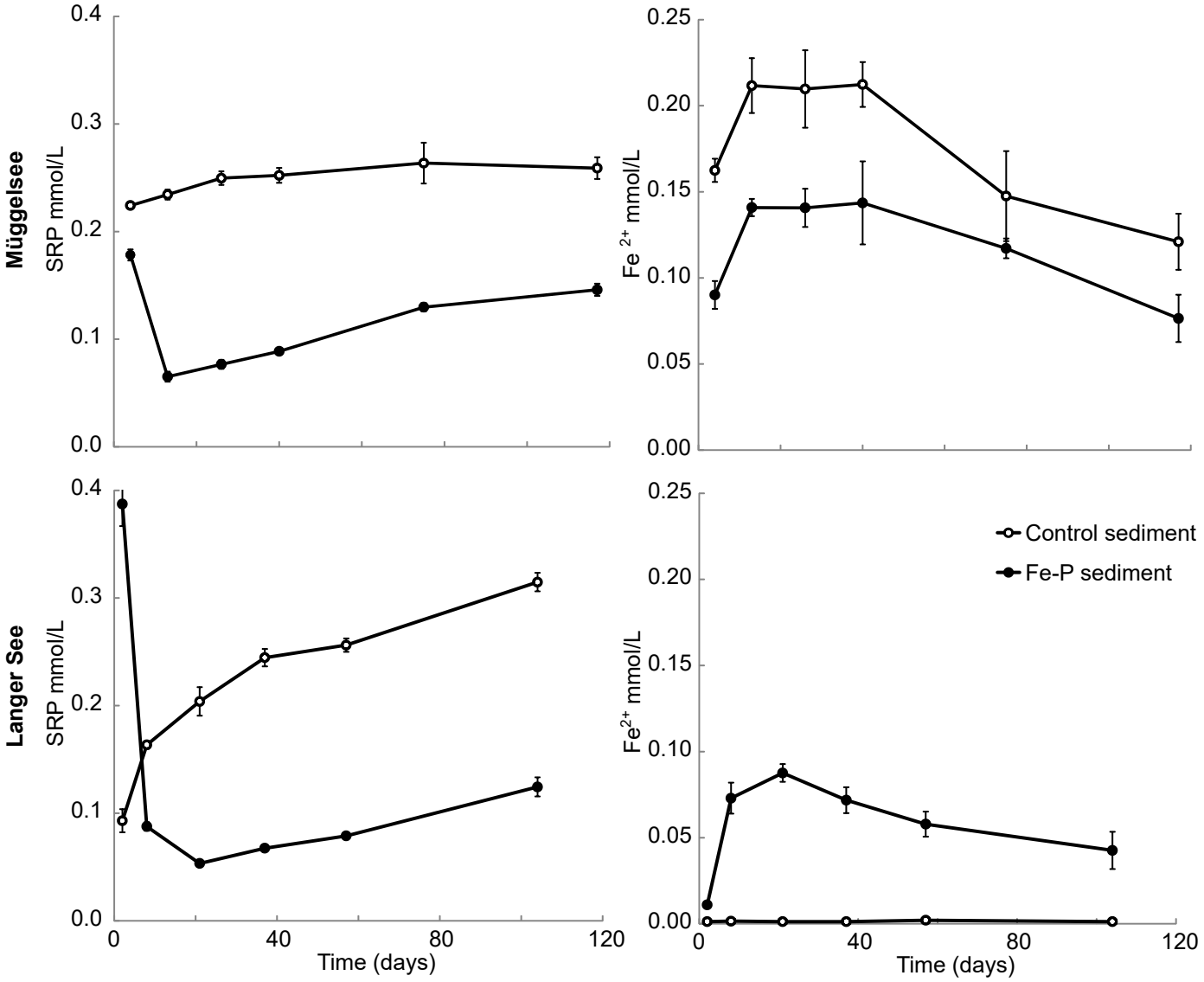

Figure 3 Pore water concentration of SRP and Fe^{2+} over time in the controls and sediments with initial addition of $Fe(OH)_3$-P from Müggelsee and Langer See (N = 4).

Figure 4

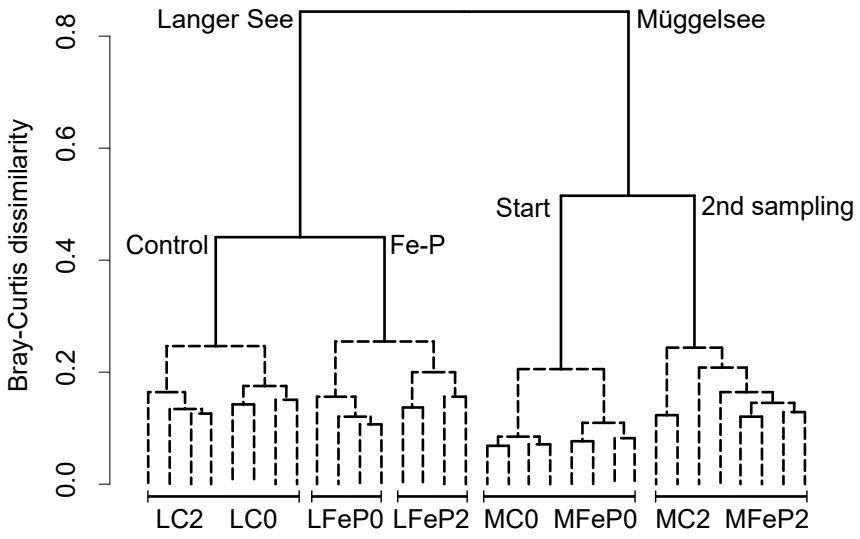

Figure 4 Dendrogram illustrating the microbial beta-diversity of the sediments initially $Fe(OH)_3$-P amended vs. the control group from Müggelsee and Langer See before anoxic incubation (start) and at the second time step when vivianite formation was observed. Cluster stability (Bray-Curtis dissimilarity, with subsequent hierarchical clustering of type complete) was tested by bootstrapping 100 times. Five stable clusters (> 0.7) were identified (continuous lines).

Electronic Supplementary Material (for online publication only)

Click here to download Electronic Supplementary Material (for online publication only): Supplementary information A.pdf